Quantum limits in interferometric detection of gravitational radiation

A. F. Pace and M. J. Collett
Department of Physics, University of Auckland, Private Bag 92019, New Zealand

D. F. Walls*
Joint Institute for Laboratory Astrophysics, University of Colorado, Boulder, Colorado 80309-0440
(Received 13 July 1992)

A spectral analysis is given of the quantum fluctuations in an optical interferometer to detect gravitational radiation. Two different methods of beating the standard quantum limit are examined: directing a squeezed state into the nonlaser input port of the interferometer and placing a Kerr medium into both arms of the interferometer. For both the Kerr medium and large squeezing cases the interferometer system is limited ultimately by the damping noise in the mirrors, not by noise in the light.

PACS number(s): 42.50.Wm, 03.65.Bz, 42.50.Lc, 42.50.Dv

I. INTRODUCTION

The determination of the fundamental quantum limits in interferometric detection of gravitational waves has been a topic of considerable debate and controversy. It has been argued that the resolution of these measurements is limited by the standard quantum limit (SQL) [1–6]. Yuen [7] has shown that the SQL may be improved using contractive states. A possible realization of such measurements has been suggested [8–10]. Caves [5–11] suggested injecting squeezed light into the empty port of the interferometer. His scheme, however, only allowed the SQL to be achieved at lower laser powers and not to be beaten. It was later shown that the SQL may be beaten by using squeezed states with an arbitrary squeezing phase [12–15]. An alternative scheme involving the insertion of a Kerr medium [16] in each arm of the interferometer was also shown to better the SQL.

In this paper we present a spectral analysis of quantum noise in an interferometer consisting of two Fabry-Pérot cavities as shown in Fig. 1. The end mirrors of each cavity are freely suspended. It is generally assumed that the mirror is practically free for frequencies that are large compared to the characteristic mirror frequency and therefore the SQL is applicable. But although at these high frequencies the mass is free from the effects of the harmonic potential well at the characteristic frequency, it is not free from the high-frequency noise terms driving the mirror, nor from the forced harmonic motion caused by the gravitational wave. Therefore we treat the mirror as a quantized harmonic oscillator. Coupling between the mirror position and the light field is introduced via radiation pressure.

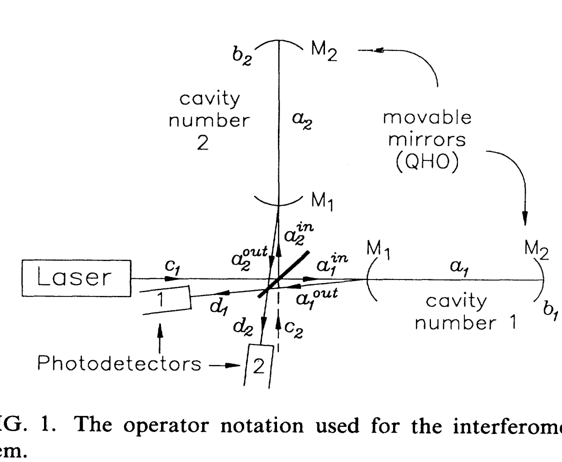

FIG. 1. The operator notation used for the interferometer system.

We begin with the Hamiltonian for a single arm of the interferometer and derive the linearized quantum Langevin equations for the output fields. This gives us the flexibility of choosing arbitrary input fields to the interferometer. The output fields from each arm of the interferometer are combined and a spectral analysis of the fluctuations in the intensity difference is given. Since both the light field and the mirror, together with their damping, are treated quantum mechanically, we are able to derive the fundamental quantum limits to the detection of a gravitational wave.

In Sec. III we demonstrate how the injection of a squeezed state into the empty port of the interferometer can be used to beat the SQL. This confirms the results of previous analyses by Unruh [12], Bondurant and Shapiro [13], Jaekel and Reynaud [14], and Luis and Sanchez-Soto [15], but from a self-consistent Hamiltonian approach. In Sec. IV we show that by inserting a Kerr medium inside both cavities the SQL may be beaten. This confirms the result of Bondurant [16], again from a self-consistent Hamiltonian approach.

II. QUANTUM NOISE ANALYSIS OF THE INTERFEROMETER

A. The system and its solution

We will begin by looking at the dynamics of a single arm of the interferometer (see Fig. 1). The cavity can be described by a Hamiltonian of the form

$$H_{\text{tot}}=H_{\text{sys}}+H_b+H_{\text{int}} \ , \tag{2.1}$$

where H_{sys} is a function of internal mode operators only, H_b is the free Hamiltonian of the baths (i.e., the external world), and H_{int} describes the interaction between the baths and internal mode operators. For the light the bath is just the external field.

In our analysis, not only is the optical cavity field quantized, but the mirror farthest away from the beam splitter, mirror M_2 (see Fig. 1), is also quantized. This means that $H_{\rm sys}$ is a function both of the cavity field mode operators and of the mirror operators. It also means that there are two baths. Both baths are assumed to consist of a continuum, in frequency, of harmonic oscillators, with each having a flat density of modes. We will assume that the coupling between each bath and its corresponding internal mode is linear.

Although the full Hamiltonian is of the form given by Eq. (2.1), in order to deduce the equations of motion for the system using a quantum Langevin equation approach [17,18], we need to consider only $H_{\rm sys}$. The cavity mode, having annihilation operator a, will be treated in an interaction picture rotating at the (laser) driving field frequency, ω_L. This is related to ω_0, the resonance frequency of the cavity in the absence of a driving field, by $\omega_0=\omega_L+\Delta$, where Δ is the detuning. The role of the detuning is to cancel the detuning produced by the mean intensity of the laser light moving the cavity mirror. The mirror is described by the mode operator b, so that $(b+b^\dagger)$ is the mirror displacement. We use

$$H_{\rm sys}=\hbar\Delta a^\dagger a+\hbar\Omega b^\dagger b+\hbar\kappa a^\dagger a(b+b^\dagger)+\hbar k s(t)(b+b^\dagger)\ . \tag{2.2}$$

The first term is the cavity detuning. The second term is the free energy of the mirror, where Ω is the characteristic angular frequency of the mirror. The third term gives the radiation pressure, where κ is the coupling constant between the cavity and mirror modes. The final term is the gravity wave, where k is the coupling constant between the classical gravity wave and the mirror mode and $s(t)$ is a function describing the time dependence of the classical gravity wave. The gravitational wave amplitude h is included in the constant k. Derivations of the coupling terms together with expressions for κ and k in terms of the parameters of the system are found in Appendices A and B, respectively.

Using the input-output theory for quantum damping [17,18], a quantum Langevin equation for each internal operator can be written as

$$\dot a=-\frac{i}{\hbar}[a,H_{\rm sys}]-\frac{\gamma_a}{2}a+\gamma_a^{1/2}a^{\rm in} \tag{2.3}$$

$$=-i[\Delta a+\kappa a(b+b^\dagger)]-\frac{\gamma_a}{2}a+\gamma_a^{1/2}a^{\rm in} \tag{2.4}$$

and

$$\dot b=-\frac{i}{\hbar}[b,H_{\rm sys}]-\frac{\gamma_b}{2}b+\gamma_b^{1/2}b^{\rm in} \tag{2.5}$$

$$=-i[\Omega b+\kappa a^\dagger a+ks(t)]-\frac{\gamma_b}{2}b+\gamma_b^{1/2}b^{\rm in}\ , \tag{2.6}$$

where γ_a is the cavity field mode damping constant (see Appendix C for an expression for γ_a in terms of the cavity parameters) and γ_b is the mirror damping constant. Owing to the approximations made in deriving Eq. (2.5), Eq. (2.6) is only valid in the low damping regime in which $\gamma_b<\Omega$.

We are working in the regime where the quantum fluctuations of the operators in Eqs. (2.4) and (2.6) are small compared to their semiclassical or deterministic part, therefore we can linearize these two equations about their semiclassical solutions. By setting all operators and parameters equal to their respective steady-state mean values and choosing the detuning Δ to be

$$\Delta=-\kappa(\beta+\beta^*)\ , \tag{2.7}$$

the following semiclassical solutions may be obtained:

$$\alpha=\frac{2\xi}{\gamma_a^{1/2}} \tag{2.8}$$

and

$$\beta=\frac{-4i\kappa|\xi|^2/\gamma_a}{\gamma_b/2+i\Omega}\ , \tag{2.9}$$

where $\langle a\rangle=\alpha$, $\langle b\rangle=\beta$, $\langle b^{\rm in}\rangle=0$, and $\langle a^{\rm in}\rangle=\xi$, where ξ is the coherent amplitude of the driving field. The gravity wave term has been treated as another small fluctuation term since $ks(t)$ has mean zero in the time domain and is of the order of the quantum fluctuations.

Linearizing Eqs. (2.4) and (2.6) for small fluctuations,

$$\begin{aligned}&a=\alpha+\delta a\ ,\quad b=\beta+\delta b\ ,\\ &a^{\rm in}=\xi+\delta a^{\rm in}\ ,\quad b^{\rm in}=\delta b^{\rm in}\ ,\end{aligned} \tag{2.10}$$

we obtain the following equations of motion, which in matrix form are

$$\frac{d}{dt}\begin{bmatrix}\delta a\\ \delta a^\dagger\\ \delta b\\ \delta b^\dagger\end{bmatrix}=-\begin{bmatrix}\frac{\gamma_a}{2} & 0 & i\kappa\alpha & i\kappa\alpha\\ 0 & \frac{\gamma_a}{2} & -i\kappa\alpha^* & -i\kappa\alpha^*\\ i\kappa\alpha^* & i\kappa\alpha & \frac{\gamma_b}{2}+i\Omega & 0\\ -i\kappa\alpha^* & -i\kappa\alpha & 0 & \frac{\gamma_b}{2}-i\Omega\end{bmatrix}\begin{bmatrix}\delta a\\ \delta a^\dagger\\ \delta b\\ \delta b^\dagger\end{bmatrix}+\begin{bmatrix}\gamma_a^{1/2}\delta a^{\rm in}\\ \gamma_a^{1/2}\delta a^{\rm in\dagger}\\ \gamma_b^{1/2}\delta b^{\rm in}\\ \gamma_b^{1/2}\delta b^{\rm in\dagger}\end{bmatrix}+\begin{bmatrix}0\\ 0\\ -iks(t)\\ +iks(t)\end{bmatrix} \tag{2.11}$$

$$\Longleftrightarrow\frac{d}{dt}\delta\mathbf{a}(t)=-\mathbf{A}\delta\mathbf{a}(t)+\mathbf{F}(t)+\mathbf{g}(t)\ . \tag{2.12}$$

The requirement for the stability of these equations is that the eigenvalues of the matrix $\mathbf{A}$ in Eq. (2.12) all have a positive real part. For all the graphs drawn in this paper the system was found to be stable.

The differental equation (2.12) is solved by transforming it into the frequency domain using the symmetric complex Fourier transform:

$$X(\omega)=\frac{1}{\sqrt{2\pi}}\int_{-\infty}^{\infty}x(t)e^{i\omega t}dt \ . \tag{2.13}$$

Solving we get

$$\delta\mathbf{a}(\omega)=(\mathbf{A}-i\omega\mathbf{I})^{-1}[\mathbf{F}(\omega)+\mathbf{g}(\omega)] \ , \tag{2.14}$$

where

$$\mathbf{F}(\omega)=\begin{bmatrix}\gamma_a^{1/2}\delta a^{\text{in}}(\omega)\\ \gamma_a^{1/2}\delta a^{\text{in}\dagger}(\omega)\\ \gamma_b^{1/2}\delta b^{\text{in}}(\omega)\\ \gamma_b^{1/2}\delta b^{\text{in}\dagger}(\omega)\end{bmatrix} , \quad \mathbf{g}(\omega=iks(\omega)\begin{bmatrix}0\\0\\-1\\+1\end{bmatrix} , \tag{2.15}$$

and

$$(\mathbf{A}-i\omega\mathbf{I})^{-1}=(\mathbf{A}-i\omega\mathbf{I})_1^{-1} \tag{2.16}$$

$$=\begin{bmatrix}\frac{\Lambda_1\Lambda_3\Lambda_4+2i\Omega\kappa^2|\alpha|^2}{\Lambda_1^2\Lambda_3\Lambda_4} & \frac{2i\Omega\kappa^2\alpha^2}{\Lambda_1^2\Lambda_3\Lambda_4} & \frac{-i\kappa\alpha}{\Lambda_1\Lambda_3} & \frac{-i\kappa\alpha}{\Lambda_1\Lambda_4}\\ \frac{-2i\Omega\kappa^2\alpha^{*2}}{\Lambda_1^2\Lambda_3\Lambda_4} & \frac{\Lambda_1\Lambda_3\Lambda_4-2i\Omega\kappa^2|\alpha|^2}{\Lambda_1^2\Lambda_3\Lambda_4} & \frac{i\kappa\alpha^*}{\Lambda_1\Lambda_3} & \frac{i\kappa\alpha^*}{\Lambda_1\Lambda_4}\\ \frac{-i\kappa\alpha^*}{\Lambda_1\Lambda_3} & \frac{-i\kappa\alpha}{\Lambda_1\Lambda_3} & \frac{1}{\Lambda_3} & 0\\ \frac{i\kappa\alpha^*}{\Lambda_1\Lambda_4} & \frac{i\kappa\alpha}{\Lambda_1\Lambda_4} & 0 & \frac{1}{\Lambda_4}\end{bmatrix} \tag{2.17}$$

where

$$\Lambda_1\equiv\Lambda_1(\omega)=\gamma_a/2-i\omega \ , \tag{2.18}$$

$$\Lambda_3\equiv\Lambda_3(\omega)=\gamma_b/2+i(\Omega-\omega) \ , \tag{2.19}$$

$$\Lambda_4\equiv\Lambda_4(\omega)=\gamma_b/2-i(\Omega+\omega) \ . \tag{2.20}$$

The notational convention that a *single digit subscript* signifies which cavity the operator or result is for is used in this paper, for example in Eq. (2.16). Please note that this does not apply to the Λ_i. We will also now introduce the notation

$$b_{ij}(\omega)=[(\mathbf{A}-i\omega\mathbf{I})_1^{-1}]_{ij} \ . \tag{2.21}$$

B. Recombining the two arms

Now that we have the solution for the internal cavity mode operators for a single arm of the interferometer (2.14), the next step is to recombine the output from the two arms assuming that the two arms have identical cavity parameters.

First, the form of the gravity wave assumed in this paper is a constant amplitude, single-frequency, sinusoidal wave propagating in a direction perpendicular to the plane of the interferometer (see Fig. 1) and hence is described mathematically by

$$s(t)=s_1(t)=\cos(\omega_g t) \ . \tag{2.22}$$

Although we have made an assumption here about the phase of $s(t)$ in order to simplify the mathematics, the results can be extended to include the effect of an arbitrary phase for $s(t)$. The two arms of the interferometer are 90° apart, so the form of the gravity wave in the second cavity is

$$s_2(t)=-s_1(t) \ , \tag{2.23}$$

since the gravity wave is a quadrupole interaction.

There is a factor of i difference between the coherent driving fields for the two cavities, which is due to the beam splitter. As the phase of ξ affects the phase of α through Eq. (2.8), the result given in Eq. (2.17) must be modified for cavity number 2. Using b_{ij} as defined in Eq. (2.21) we get

$$(\mathbf{A}-i\omega\mathbf{I})_2^{-1}=\begin{bmatrix}b_{11} & -b_{12} & ib_{13} & ib_{14}\\ -b_{21} & b_{22} & -ib_{23} & -ib_{24}\\ -ib_{31} & ib_{32} & b_{33} & b_{34}\\ -ib_{41} & ib_{42} & b_{43} & b_{44}\end{bmatrix} . \tag{2.24}$$

The next step is to get an expression for the cavity output light fields in terms of the input fields of the system. The mirror boundary condition is [17,18]

$$\delta a^{\text{out}}(\omega)=\gamma_a^{1/2}\delta a(\omega)-\delta a^{\text{in}}(\omega) \ . \tag{2.25}$$

Therefore, using the notation in Fig. 1, the output fields of interest are (in matrix form)

$$\begin{bmatrix} \delta a_1^{\text{out}}(\omega) \\ \delta a_1^{\text{out}\dagger}(\omega) \\ \delta a_2^{\text{out}}(\omega) \\ \delta a_2^{\text{out}\dagger}(\omega) \end{bmatrix} = \gamma_a^{1/2} \begin{bmatrix} \delta a_1(\omega) \\ \delta a_1^\dagger(\omega) \\ \delta a_2(\omega) \\ \delta a_2^\dagger(\omega) \end{bmatrix} - \begin{bmatrix} \delta a_1^{\text{in}}(\omega) \\ \delta a_1^{\text{in}\dagger}(\omega) \\ \delta a_2^{\text{in}}(\omega) \\ \delta a_2^{\text{in}\dagger}(\omega) \end{bmatrix} \quad (2.26)$$

$$\Longrightarrow \delta \mathbf{a}_{12}^{\text{out}}(\omega) = \gamma_a^{1/2} \delta \mathbf{a}_{12}(\omega) - \delta \mathbf{a}_{12}^{\text{in}}(\omega) \ , \quad (2.27)$$

where we have used the subscript 12 to indicate that the vector contains operators from both cavities.

Let

$$\delta \mathbf{a}_i^{\text{in}}(\omega) = \begin{bmatrix} \delta a_i^{\text{in}}(\omega) \\ \delta a_i^{\text{in}\dagger}(\omega) \\ \delta b_i^{\text{in}}(\omega) \\ \delta b_i^{\text{in}\dagger}(\omega) \end{bmatrix} , \quad (2.28)$$

where $i=1$ or 2. Then Eq. (2.27) can be written as

$$\delta \mathbf{a}_{12}^{\text{out}}(\omega) = \mathbf{M}_{10}(\omega) \delta \mathbf{a}_1^{\text{in}}(\omega) + \mathbf{M}_{02}(\omega) \delta \mathbf{a}_2^{\text{in}}(\omega) + \mathbf{g}(\omega) \ , \quad (2.29)$$

where

$$\mathbf{M}_{10}(\omega) = \begin{bmatrix} \gamma_a b_{11}(\omega) - 1 & \gamma_a b_{12}(\omega) & (\gamma_a \gamma_b)^{1/2} b_{13}(\omega) & (\gamma_a \gamma_b)^{1/2} b_{14}(\omega) \\ \gamma_a b_{21}(\omega) & \gamma_a b_{22}(\omega) - 1 & (\gamma_a \gamma_b)^{1/2} b_{23}(\omega) & (\gamma_a \gamma_b)^{1/2} b_{24}(\omega) \\ 0 & 0 & 0 & 0 \\ 0 & 0 & 0 & 0 \end{bmatrix} , \quad (2.30)$$

$$\mathbf{M}_{02}(\omega) = \begin{bmatrix} 0 & 0 & 0 & 0 \\ 0 & 0 & 0 & 0 \\ \gamma_a b_{11}(\omega) - 1 & -\gamma_a b_{12}(\omega) & i(\gamma_a \gamma_b)^{1/2} b_{13}(\omega) & i(\gamma_a \gamma_b)^{1/2} b_{14}(\omega) \\ -\gamma_a b_{21}(\omega) & \gamma_a b_{22}(\omega) - 1 & -i(\gamma_a \gamma_b)^{1/2} b_{23}(\omega) & -i(\gamma_a \gamma_b)^{1/2} b_{24}(\omega) \end{bmatrix} , \quad (2.31)$$

and

$$\mathbf{g}(\omega) = \gamma_a^{1/2} k s(\omega) \begin{bmatrix} i[b_{14}(\omega) - b_{13}(\omega)] \\ i[b_{24}(\omega) - b_{23}(\omega)] \\ [b_{14}(\omega) - b_{13}(\omega)] \\ -[b_{24}(\omega) - b_{23}(\omega)] \end{bmatrix} . \quad (2.32)$$

C. The performance of the system

Our aim is to determine the minimum possible gravitational wave amplitude h that this particular interferometer system can detect. In order to do this we need first to determine the signal and its variance.

In Fig. 1 we have two ideal photodetectors at the output which count the number of photons incident on them. Let the intensity of light (measured in photons per second) reaching photodetector 1 be I_1 and that reaching photodetector 2, I_2. Then the signal and variance are, in the frequency domain,

$$\mathcal{S}(\omega) = \langle I_1(\omega) - I_2(\omega) \rangle \quad (2.33)$$

and

$$\mathcal{V} = \langle I_1(\omega) - I_2(\omega), I_1(\omega') - I_2(\omega') \rangle \ . \quad (2.34)$$

As the variance when expressed directly in terms of boson annihilation and creation operators is a linear combination of fourth-order moments, a large intensity approximation will be made. This reduces the moments to second order. Making a substitution of variables for a_1^{out} and a_2^{out} (see Fig. 1),

$$a_1^{\text{out}}(t) = (I_1^{\text{out}})^{1/2} e^{i\phi_1} \ , \quad (2.35)$$

$$a_2^{\text{out}}(t) = (I_2^{\text{out}})^{1/2} e^{i\phi_2} \ , \quad (2.36)$$

and taking advantage of the beam splitter, we get

$$\begin{aligned} I_1(t) - I_2(t) &= d_1^\dagger d_1 - d_2^\dagger d_2 \\ &= 2(I_1^{\text{out}} I_2^{\text{out}})^{1/2} \sin(\phi_1 - \phi_2) \\ &\approx 2I \sin(\phi_1 - \phi_2) \ , \end{aligned} \quad (2.37)$$

where I_1^{out} and I_2^{out} have each been replaced by their mean value:

$$\langle I_1^{\text{out}} \rangle = \langle I_2^{\text{out}} \rangle = |\xi|^2 = I \ , \quad (2.38)$$

which is valid for large I.

Now a phase shift ϕ is introduced between cavity number 1 and the beam splitter such that

$$\langle \phi_1 - \phi_2 \rangle + \phi = 0 \ , \quad (2.39)$$

which balances the outputs I_1 and I_2. This means that both of the interferometer outputs are sitting halfway between a dark fringe and a bright fringe. Therefore we get

$$\begin{aligned} I_1(t) - I_2(t) &= 2I \sin(\phi_1 + \phi - \phi_2) \\ &= 2I \sin(\delta\phi_1 - \delta\phi_2) \\ &\approx 2I(\delta\phi_1 - \delta\phi_2) \ , \end{aligned} \quad (2.40)$$

where the last line follows from the fact that $\delta\phi_1 - \delta\phi_2$ is small for $I \gg 1$.

As a result of the beam splitter, $\langle \phi_2 \rangle = \langle \phi_1 \rangle + \pi/2$. We have arbitrarily set $\langle \phi_1 \rangle = 0$ which is equivalent to assuming that ξ is real and hence also α [see Eq. (2.8)]. Choosing an arbitrary phase for ξ does not change the final results but only makes the intermediate results more complicated. We have

$$\delta\phi_1 \approx \frac{X_2}{\langle X_1 \rangle} , \quad = \frac{i}{2\sqrt{I}}(\delta a_1^{\text{out}\dagger} - \delta a_1^{\text{out}}) , \tag{2.41}$$

$$\delta\phi_2 \approx \frac{-X_1}{\langle X_2 \rangle} , \quad = \frac{-1}{2\sqrt{I}}(\delta a_2^{\text{out}\dagger} + \delta a_2^{\text{out}}) , \tag{2.42}$$

which gives

$$I_1(t) - I_2(t) = \sqrt{I}\,\{ i[\delta a_1^{\text{out}\dagger}(t) - \delta a_1^{\text{out}}(t)] + [\delta a_2^{\text{out}\dagger}(t) + \delta a_2^{\text{out}}(t)]\} . \tag{2.43}$$

Transforming Eq. (2.43) into the frequency domain yields

$$I_1(\omega) - I_2(\omega) = \sqrt{I}\,\{ i[\delta a_1^{\text{out}\dagger}(\omega) - \delta a_1^{\text{out}}(\omega)] + [\delta a_2^{\text{out}\dagger}(\omega) + \delta a_2^{\text{out}}(\omega)]\} . \tag{2.44}$$

Therefore, using Eq. (2.29) the signal is

$$\mathcal{S} = \langle I_1(\omega) - I_2(\omega) \rangle \tag{2.45}$$

$$= 2(I\gamma_a)^{1/2} ks(\omega)[b_{14}(\omega) - b_{13}(\omega) + b_{23}(\omega) - b_{24}(\omega)] \tag{2.46}$$

$$= \frac{32h\omega_g^2\omega_0 s(\omega) I}{\Lambda_1(\omega)\Lambda_3(\omega)\Lambda_4(\omega)} , \tag{2.47}$$

where the $\Lambda_i(\omega)$ are defined in Eqs. (2.18)–(2.20), and Eqs. (2.8), (2.38), (A13), and (B10) have been used.

A useful quantity in calculating the variance is the output field correlation matrix $\mathbf{C}(\omega)$, defined by

$$\mathbf{C}(\omega) = \langle \delta\mathbf{a}_{12}^{\text{out}}(\omega), \delta\mathbf{a}_{12}^{\text{out}\,T}(\omega') \rangle \tag{2.48}$$

$$= \mathbf{M}_{10}(\omega)\langle \delta\mathbf{a}_1^{\text{in}}(\omega)\delta\mathbf{a}_1^{\text{in}\,T}(\omega')\rangle \mathbf{M}_{10}^T(\omega') + \mathbf{M}_{02}(\omega)\langle \delta\mathbf{a}_2^{\text{in}}(\omega)\delta\mathbf{a}_1^{\text{in}\,T}(\omega')\rangle \mathbf{M}_{10}^T(\omega')$$
$$+ \mathbf{M}_{10}(\omega)\langle \delta\mathbf{a}_1^{\text{in}}(\omega)\delta\mathbf{a}_2^{\text{in}\,T}(\omega')\rangle M_{02}^T(\omega') + \mathbf{M}_{02}(\omega)\langle \delta\mathbf{a}_2^{\text{in}}(\omega)\delta\mathbf{a}_2^{\text{in}\,T}(\omega')\rangle M_{02}^T(\omega') . \tag{2.49}$$

The variance can be written as

$$\mathcal{V} = \langle I_1(\omega) - I_2(\omega), I_1(\omega') - I_2(\omega') \rangle \tag{2.50}$$

$$= I[c_{33} - c_{11} + c_{44} - c_{22} + c_{12} + c_{34} + c_{21} + c_{43} - i(c_{13} + c_{31}) - i(c_{14} - c_{32}) + i(c_{23} - c_{41}) + i(c_{24} + c_{42})] . \tag{2.51}$$

Now that we have expressions for the signal and variance, the next step is to optimize the detectability of the gravitational wave amplitude h with respect to laser power.

The signal and variance can be written in the form

$$\mathcal{S}(\omega) = f_s(\omega) hs(\omega) \tag{2.52}$$

and

$$\mathcal{V}(\omega) = f_v(\omega)\delta(\omega + \omega') , \tag{2.53}$$

where $f_v(\omega)$ is commonly called the *power spectral density*. Signal processing theory [19] tells us that for a measurement of a signal at a frequency ω_g the uncertainty in the measurement of $h, \Delta h$, is given by

$$\Delta h = \frac{[f_v(\omega_g)]^{1/2}}{|f_s(\omega_g)|}\frac{1}{\sqrt{\tau/2}} , \tag{2.54}$$

where it is assumed that the measurement time τ is much greater than the period of the gravity wave. Δh is assumed to define the lower limit on the size of the detectable gravitational wave amplitude h, so we have

$$h = h_{\min} = \Delta h . \tag{2.55}$$

Now I is related to the laser power P by

$$P = 2\hbar\omega_0 I . \tag{2.56}$$

As $f_s(\omega)$ and $f_v(\omega)$ will be expressed in terms of I and not P, it is easier to do the minimization with respect to I and then to use Eq. (2.56) to find the optimum power. It is also easier mathematically to minimize h^2 rather than h, where

$$h^2 = \frac{2f_v(\omega_g)}{\tau|f_s(\omega_g)|^2} . \tag{2.57}$$

D. Application to a vacuum input

In order to calculate the variance, the input field correlations in Eq. (2.49) need to be determined. Up until now the input fields to the interferometer have been kept arbitrary. We now assume that our input light fields, c_1 and c_2 (see Fig. 1), are a coherent state (laser input) and an unsqueezed vacuum, respectively. The input mirror modes, δb_1^{in} and δb_2^{in}, will also be assumed to be unsqueezed vacuum states. The input light fields are assumed to be independent of the input mirror modes. As before, the thermal fluctuations in all the input field correlations will be neglected. With these assumptions, $\delta\mathbf{a}_1^{\text{in}}$ and $\delta\mathbf{a}_2^{\text{in}}$ are independent of each other:

$$\langle \delta\mathbf{a}_1^{\text{in}}(\omega)\delta\mathbf{a}_2^{\text{in}\,T}(\omega')\rangle = \langle \delta\mathbf{a}_2^{\text{in}}(\omega)\delta\mathbf{a}_1^{\text{in}\,T}(\omega')\rangle = \mathbf{0} , \tag{2.58}$$

and the other correlations are

$$\langle \delta \mathbf{a}_1^{\text{in}}(\omega)\delta \mathbf{a}_1^{\text{in}T}(\omega')\rangle = \langle \delta \mathbf{a}_2^{\text{in}}(\omega)\delta \mathbf{a}_2^{\text{in}T}(\omega')\rangle = \begin{bmatrix} 0 & 1 & 0 & 0 \\ 0 & 0 & 0 & 0 \\ 0 & 0 & 0 & 1 \\ 0 & 0 & 0 & 0 \end{bmatrix} \delta(\omega+\omega') . \quad (2.59)$$

Using Eqs. (2.58) and (2.59) and letting

$$c_{ij} = [\mathbf{C}(\omega)]_{ij} , \quad (2.60)$$

the following results are obtained for the components of $\mathbf{C}(\omega)$:

$$c_{11} = -c_{33} = \{[\gamma_a b_{11}(\omega) - 1]\gamma_a b_{12}(\omega') + \gamma_a \gamma_b b_{13}(\omega) b_{14}(\omega')\}\delta(\omega+\omega') , \quad (2.61)$$

$$c_{12} = c_{34} = \{[\gamma_a b_{11}(\omega) - 1][\gamma_a b_{22}(\omega') - 1] + \gamma_a \gamma_b b_{13}(\omega) b_{24}(\omega')\}\delta(\omega+\omega') , \quad (2.62)$$

$$c_{21} = c_{43} = [\gamma_a^2 b_{21}(\omega) b_{12}(\omega') + \gamma_a \gamma_b b_{23}(\omega) b_{14}(\omega')]\delta(\omega+\omega') , \quad (2.63)$$

$$c_{22} = -c_{44} = \{\gamma_a b_{21}(\omega)[\gamma_a b_{22}(\omega') - 1] + \gamma_a \gamma_b b_{23}(\omega) b_{24}(\omega')\}\delta(\omega+\omega') , \quad (2.64)$$

$$c_{13} = c_{14} = c_{23} = c_{24} = c_{31} = c_{32} = c_{41} = c_{42} = 0 . \quad (2.65)$$

So expanding out the variance in Eq. (2.51) and simplifying, we get

$$\mathcal{V} = 2I\left[1 + \frac{16\kappa^2\gamma_b[(\gamma_b/2)^2 + \Omega^2 + \omega^2]I}{|\Lambda_1(\omega)|^2|\Lambda_3(\omega)|^2|\Lambda_4(\omega)|^2} + \frac{(16\Omega\kappa^2)^2 I^2}{|\Lambda_1(\omega)|^4|\Lambda_3(\omega)|^2|\Lambda_4(\omega)|^2}\right]\delta(\omega+\omega') , \quad (2.66)$$

where the $\Lambda_i(\omega)$ are defined in Eqs. (2.18)–(2.20).

The variance can also be expressed in units in which the vacuum noise level is 1. This particular variance, which will be denoted by a subscript *vnl*, is defined by

$$\mathcal{V} = 2I\mathcal{V}_{vnl}\delta(\omega+\omega') . \quad (2.67)$$

Therefore Eq. (2.66) becomes

$$\mathcal{V}_{vnl} = 1 + \frac{16\kappa^2\gamma_b[(\gamma_b/2)^2 + \Omega^2 + \omega^2]I}{|\Lambda_1(\omega)|^2|\Lambda_3(\omega)|^2|\Lambda_4(\omega)|^2} + \frac{(16\Omega\kappa^2)^2 I^2}{|\Lambda_1(\omega)|^4|\Lambda_3(\omega)|^2|\Lambda_4(\omega)|^2} . \quad (2.68)$$

Let us now examine the different noise terms in Eq. (2.66). The first term is the photon counting noise which is produced by the intrinsic phase fluctuations of the light field mode *inside* the cavity. It is apparent from Eq. (2.40) that the phase fluctuations will appear in the output signal. The second term is the mirror noise. It is a direct consequence of treating the mirror as a quantum harmonic oscillator damped to a white-noise bath. This white-noise bath produces frequency-independent fluctuations in the mirror's momentum which in turn produce small phase changes in the cavity light field and hence fluctuations in the output signal. The third term is the radiation pressure noise, which is produced by the intrinsic intensity fluctuations of the light field mode *inside* the cavity. The mirror is driven by these fluctuations in exactly the same way as a mass on a spring is driven by an external driving force. These fluctuations in the mirror displacement produce small phase changes in the cavity light field which, in turn, are detected at the output.

Figure 2 shows a graph of the spectrum of the variance expressed in units in which the vacuum noise level is 1. The graph shows not only the total variance (solid line), but the contribution of each term in Eq. (2.68) to the total. The values chosen for the experimental parameters are shown in Table I; they are estimates for a small-scale or prototype interferometer. For the particular laser power chosen, the variance is dominated by the radiation pressure noise for frequencies small compared with the mirror resonance frequency. In this frequency regime the mirror fluctuations are dominated by the radiation pressure noise. At frequencies much higher than the mirror resonance frequency the variance is dominated by the photon counting noise. In this frequency regime the mir-

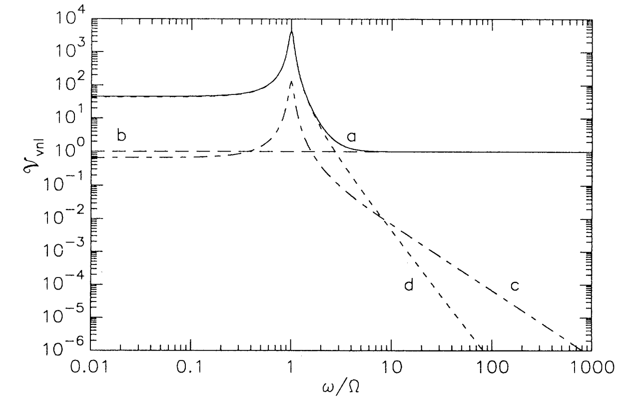

FIG. 2. (Curve *a*) The total noise, $\mathcal{V}_{vnl}$ (solid line). Contributions to $\mathcal{V}_{vnl}$: (curve *b*) photon counting noise (dashed line); (curve *c*) mirror noise (dash-dotted line); (curve *d*) radiation pressure noise (dotted line).

TABLE I. The values of the experimental parameters used in the graphs.

Quantity	Symbol	Value
Mass of mirror	M	10 kg
Mirror characteristic angular frequency	Ω	20π rad s^{-1}
Mirror damping	γ_b	2π rad s^{-1}
Length of cavity	L	4 m
Reflectivity of mirror M_1	R	0.98
Laser power	P	10 W
Laser angular frequency	ω_0	3.66×10^{15} rad s^{-1}
Gravity wave angular frequency	ω_g	2000π rad s^{-1}

ror is less responsive to the radiation pressure driving field and is also almost out of phase with it. Both the radiation pressure noise and the mirror noise depend directly on the frequency response of the mirror to a driving field and hence both have the characteristic response spectrum for forced harmonic motion superimposed on them.

Now the signal and variance can be written in the form of Eqs. (2.52) and (2.53), where

$$f_s(\omega)=\frac{32\omega_g^2\omega_0 I}{\Lambda_1(\omega)\Lambda_3(\omega)\Lambda_4(\omega)} \tag{2.69}$$

and

$$f_v(\omega)=2I\left[1+\frac{16\kappa^2\gamma_b[(\gamma_b/2)^2+\Omega^2+\omega^2]I}{|\Lambda_1(\omega)|^2|\Lambda_3(\omega)|^2|\Lambda_4(\omega)|^2}+\frac{(16\Omega\kappa^2)^2I^2}{|\Lambda_1(\omega)|^4|\Lambda_3(\omega)|^2|\Lambda_4(\omega)|^2}\right] . \tag{2.70}$$

Substituting $f_s(\omega)$ and $f_v(\omega)$ back into Eq. (2.57) yields

$$h^2=f(\omega_g)[1/I+f_1(\omega_g)+f_2(\omega_g)I] , \tag{2.71}$$

where

$$f(\omega)=\frac{|\Lambda_1(\omega)|^2|\Lambda_3(\omega)|^2|\Lambda_4(\omega)|^2}{\tau[16\omega_g^2\omega_0]^2} , \tag{2.72}$$

$$f_1(\omega)=\frac{16\kappa^2\gamma_b[(\gamma_b/2)^2+\Omega^2+\omega^2]}{|\Lambda_1(\omega)|^2|\Lambda_3(\omega)|^2|\Lambda_4(\omega)|^2} , \tag{2.73}$$

$$f_2(\omega)=\frac{(16\Omega\kappa^2)^2}{|\Lambda_1(\omega)|^4|\Lambda_3(\omega)|^2|\Lambda_4(\omega)|^2} . \tag{2.74}$$

The minimum value of h^2 occurs for an optimum intensity

$$I_{\rm opt}=\frac{1}{[f_2(\omega_g)]^{1/2}} , \tag{2.75}$$

and hence the optimum laser power is

$$P_{\rm opt}=2\hbar\omega_0 I_{\rm opt}=P_0 . \tag{2.76}$$

Substituting $I_{\rm opt}$ back into Eq. (2.71) gives

$$h^2_{\rm min}=f(\omega_g)\{2[f_2(\omega_g)]^{1/2}+f_1(\omega_g)\} . \tag{2.77}$$

Figure 3 shows a graph of the square root of Eq. (2.71)

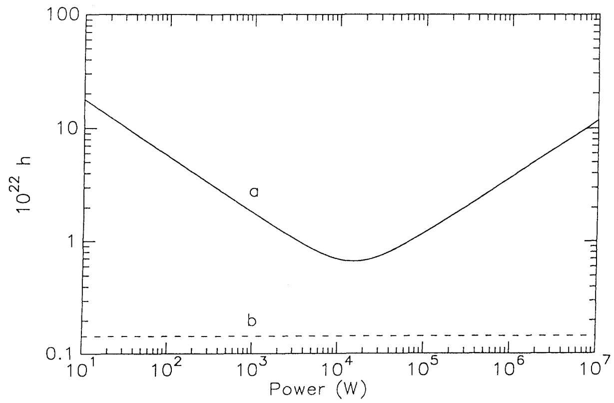

FIG. 3. (Curve *a*) The minimum possible gravitational wave amplitude *h* detectable as a function of power. (Curve *b*) The contribution of the mirror noise to *h*.

where a measurement time of $\tau=1$ s has been assumed and the values in Table I have been used. The contribution of the mirror noise to h has been included for comparative purposes.

In the frequency regime in which we are interested,

$$\omega_g^2 \gg \left[\frac{\gamma_b}{2}\right]^2+\Omega^2 \tag{2.78}$$

so that Eq. (3.37) reduces to

$$h^2_{\rm min}\approx\frac{\hbar}{8M\omega_g^2L^2\tau\Omega}[2\Omega+\gamma_b] . \tag{2.79}$$

The first term in the square brackets can be traced back to the quantum-mechanical uncertainties in the light and the second term comes directly from treating the mirror as a quantum harmonic oscillator damped to a white-noise bath.

Now most analyses obtain the standard quantum limit by considering only the effect of noise sources due to the light field. So if we are to compare our expression for the SQL with that of others, we should focus on the term due to the quantum-mechanical uncertainties in the light. From the first term in Eq. (2.79) we get

$$h_{\rm SQL}=\frac{1}{L}\left[\frac{\hbar}{4M\omega_g^2\tau}\right]^{1/2} . \tag{2.80}$$

The functional form of this result agrees with that of Edelstein *et al.* [4].

III. SQUEEZING

In this section we consider the specific case of a squeezed state entering the empty port of the interferometer. The results in the first three subsections of Sec. II are valid for arbitrary input fields. In order to calculate the variance, the input field correlations in Eq. (2.49) need to be determined for this particular case.

A. Input field correlations

From Fig. 1 we have the beam-splitter relation

$$\begin{pmatrix} a_1^{\rm in} \\ a_2^{\rm in} \end{pmatrix} = \frac{1}{\sqrt{2}} \begin{pmatrix} 1 & i \\ i & 1 \end{pmatrix} \begin{pmatrix} c_1 \\ c_2 \end{pmatrix}, \tag{3.1}$$

where c_1 is a coherent state (laser input) and c_2 is a squeezed state. In order to describe these states we will use the unitary displacement operator [20] and the unitary squeeze operator [21,22], defined, respectively, by

$$D(\xi_L) = \exp(\xi_L c_1'^\dagger - \xi_L^* c_1') \tag{3.2}$$

and

$$S(\epsilon) = \exp[\tfrac{1}{2}(\epsilon^* c_2'^2 - \epsilon c_2'^{\dagger 2})], \tag{3.3}$$

where ξ_L is the mean amplitude of the laser and $\epsilon = re^{i\theta}$ is a complex number which indicates both the magnitude and phase of the squeezing, the latter being measured relative to the phase of ξ_L.

So we have

$$c_1 = D^\dagger(\xi_L) c_1' D(\xi_L) = c_1' + \xi_L \tag{3.4}$$

and

$$c_2 = S^\dagger(\epsilon) c_2' S(\epsilon) = c_2' \cosh r - c_2'^\dagger e^{i\theta} \sinh r . \tag{3.5}$$

Now defining $\delta a_1^{\rm in}$ and $\delta a_2^{\rm in}$ as

$$\delta a_1^{\rm in} = a_1^{\rm in} - \langle a_1^{\rm in} \rangle = a_1^{\rm in} - \xi , \tag{3.6}$$

$$\delta a_2^{\rm in} = a_2^{\rm in} - \langle a_2^{\rm in} \rangle = a_2^{\rm in} - i\xi , \tag{3.7}$$

where $\xi = (1/\sqrt{2})\xi_L$, and transferring them from the time domain into the frequency domain, we get

$$\begin{pmatrix} \delta a_1^{\rm in}(\omega) \\ \delta a_1^{\rm in\dagger}(\omega) \\ \delta a_2^{\rm in}(\omega) \\ \delta a_2^{\rm in\dagger}(\omega) \end{pmatrix} = \frac{1}{\sqrt{2}} \begin{pmatrix} 1 & 0 & i\cosh r & -ie^{i\theta}\sinh r \\ 0 & 1 & ie^{-i\theta}\sinh r & -i\cosh r \\ i & 0 & \cosh r & -e^{i\theta}\sinh r \\ 0 & -i & -e^{-i\theta}\sinh r & \cosh r \end{pmatrix} \begin{pmatrix} c_1(\omega) \\ c_1^\dagger(\omega) \\ c_2(\omega) \\ c_2^\dagger(\omega) \end{pmatrix} \tag{3.8}$$

$$\Longleftrightarrow \delta \mathbf{a}_{12}^{\rm in}(\omega) = \mathbf{M}(\omega)\mathbf{c}(\omega) , \tag{3.9}$$

where the $1/\sqrt{2}$ factor is included in the matrix $\mathbf{M}(\omega)$.

Neglecting thermal fluctuations in the input light field correlations, we get

$$\langle \mathbf{c}(\omega)\mathbf{c}(\omega')^T \rangle = \begin{pmatrix} 0 & 1 & 0 & 0 \\ 0 & 0 & 0 & 0 \\ 0 & 0 & 0 & 1 \\ 0 & 0 & 0 & 0 \end{pmatrix} \delta(\omega+\omega') . \tag{3.10}$$

The input field correlation matrix is

$$\langle \delta\mathbf{a}_{12}^{\rm in}(\omega) \delta\mathbf{a}_{12}^{{\rm in}T}(\omega') \rangle = \mathbf{M} \langle \mathbf{c}(\omega)\mathbf{c}(\omega')^T \rangle \mathbf{M}^T \tag{3.11}$$

$$= \mathbf{C}^{\rm in}\delta(\omega+\omega') , \tag{3.12}$$

where

$$\mathbf{C}^{\rm in} = \frac{1}{2} \begin{vmatrix} M & N+2 & -iM & iN \\ N & M^* & -iN & iM^* \\ -iM & -iN & -M & N+2 \\ iN & iM^* & N & -M^* \end{vmatrix} , \tag{3.13}$$

and where $N = \sinh^2 r$ and $M = \frac{1}{2} e^{i\theta} \sinh 2r$.

The mirror inputs are, of course, independent of the input light fields. And we will neglect thermal fluctuations in the mirror inputs so that the only nonzero correlations between them are

$$\langle \delta b_1^{\rm in} \delta b_1^{\rm in\dagger} \rangle = \langle \delta b_2^{\rm in} \delta b_2^{\rm in\dagger} \rangle = \delta(\omega+\omega') . \tag{3.14}$$

Thermal fluctuations in the mirror are, at present, one of the dominant experimental noise sources. It is possible to extend our results to include them, but here we are only interested in investigating the fundamental quantum limits of the problem.

Having determined the input field correlations in Eq. (2.49) we can now find the output field correlation matrix $\mathbf{C}(\omega)$. Letting

$$c_{ij} = [\mathbf{C}(\omega)]_{ij} \tag{3.15}$$

and

$$c_{ij}^{\rm in} = [\mathbf{C}^{\rm in}]_{\rm ij} , \tag{3.16}$$

the components of $\mathbf{C}(\omega)$ are

$$c_{11} = -c_{33} = \{ [c_{11}^{\rm in}(\gamma_a b_{11}(\omega) - 1) + c_{21}^{\rm in}\gamma_a b_{12}(\omega)][\gamma_a b_{11}(\omega') - 1] + [c_{12}^{\rm in}(\gamma_a b_{11}(\omega) - 1) + c_{22}^{\rm in}\gamma_a b_{12}(\omega)]\gamma_a b_{12}(\omega') + \gamma_a\gamma_b b_{13}(\omega) b_{14}(\omega') \} \delta(\omega+\omega') , \tag{3.17}$$

$$c_{22} = -c_{44} = \{ [c_{12}^{\rm in}\gamma_a b_{21}(\omega) + c_{22}^{\rm in}(\gamma_a b_{22}(\omega) - 1)][\gamma_a b_{22}(\omega') - 1] + [c_{11}^{\rm in}\gamma_a b_{21}(\omega) + c_{21}^{\rm in}(\gamma_a b_{22}(\omega) - 1)]\gamma_a b_{21}(\omega') + \gamma_a\gamma_b b_{23}(\omega) b_{24}(\omega') \} \delta(\omega+\omega') , \tag{3.18}$$

$$c_{12}=c_{34}=\{[c_{12}^{\text{in}}(\gamma_a b_{11}(\omega)-1)+c_{22}^{\text{in}}\gamma_a b_{12}(\omega)][\gamma_a b_{22}(\omega')-1]$$
$$+[c_{11}^{\text{in}}(\gamma_a b_{11}(\omega)-1)+c_{21}^{\text{in}}\gamma_a b_{12}(\omega)]\gamma_a b_{21}(\omega')+\gamma_a\gamma_b b_{13}(\omega)b_{24}(\omega')\}\delta(\omega+\omega') , \tag{3.19}$$

$$c_{21}=c_{43}=\{[c_{11}^{\text{in}}\gamma_a b_{21}(\omega)+c_{21}^{\text{in}}(\gamma_a b_{22}(\omega)-1)][\gamma_a b_{11}(\omega')-1]$$
$$+[c_{12}^{\text{in}}\gamma_a b_{21}(\omega)+c_{22}^{\text{in}}(\gamma_a b_{22}(\omega)-1)]\gamma_a b_{12}(\omega')+\gamma_a\gamma_b b_{23}(\omega)b_{14}(\omega')\}\delta(\omega+\omega') , \tag{3.20}$$

$$c_{13}=c_{31}=\{[c_{13}^{\text{in}}(\gamma_a b_{11}(\omega)-1)+c_{23}^{\text{in}}\gamma_a b_{12}(\omega)][\gamma_a b_{11}(\omega')-1]$$
$$-[c_{14}^{\text{in}}(\gamma_a b_{11}(\omega)-1)+c_{24}^{\text{in}}\gamma_a b_{12}(\omega)]\gamma_a b_{12}(\omega')\}\delta(\omega+\omega') , \tag{3.21}$$

$$c_{24}=c_{42}=\{-[c_{13}^{\text{in}}\gamma_a b_{21}(\omega)+c_{23}^{\text{in}}(\gamma_a b_{22}(\omega)-1)]\gamma_a b_{21}(\omega')$$
$$+[c_{14}^{\text{in}}\gamma_a b_{24}(\omega)+c_{22}^{\text{in}}(\gamma_a b_{22}(\omega)-1)][\gamma_a b_{22}(\omega')-1]\}\delta(\omega+\omega') , \tag{3.22}$$

$$c_{14}=-c_{32}=\{-[c_{13}^{\text{in}}(\gamma_a b_{11}(\omega)-1)+c_{23}^{\text{in}}\gamma_a b_{12}(\omega)]\gamma_a b_{21}(\omega')$$
$$+[c_{14}^{\text{in}}(\gamma_a b_{11}(\omega)-1)+c_{24}^{\text{in}}\gamma_a b_{12}(\omega)][\gamma_a b_{22}(\omega')-1]\}\delta(\omega+\omega') , \tag{3.23}$$

$$c_{23}=-c_{41}=\{[c_{13}^{\text{in}}\gamma_a b_{21}(\omega)+c_{23}^{\text{in}}(\gamma_a b_{22}(\omega)-1)][\gamma_a b_{11}(\omega')-1]$$
$$-[c_{14}^{\text{in}}\gamma_a b_{21}(\omega)+c_{24}^{\text{in}}(\gamma_a b_{22}(\omega)-1)]\gamma_a b_{12}(\omega')\}\delta(\omega+\omega') . \tag{3.24}$$

B. Evaluating the performance of the system

The variance in Eq. (2.51) can now be expanded and simplified to give

$$\mathcal{V}=2I\left[(\cosh 2r_2-\cos\theta\sinh 2r_2)+\frac{16\kappa^2\gamma_b[(\gamma_b/2)^2+\Omega^2+\omega^2]I}{|\Lambda_1(\omega)|^2|\Lambda_3(\omega)|^2|\Lambda_4(\omega)|^2}+\frac{\sinh 2r_2\sin\theta\, 32\Omega\kappa^2[(\gamma_b/2)^2+\Omega^2-\omega^2]I}{|\Lambda_1(\omega)|^2|\Lambda_3(\omega)|^2|\Lambda_4(\omega)|^2}\right.$$
$$\left.+\frac{(\cosh 2r_2+\cos\theta\sinh 2r_2)(16\Omega\kappa^2)^2I^2}{|\Lambda_1(\omega)|^4|\Lambda_3(\omega)|^2|\Lambda_4(\omega)|^2}\right]\delta(\omega+\omega') \tag{3.25}$$
$$=2I[\sin\theta g_1(\omega)+\cos\theta g_2(\omega)+g_3(\omega)]\delta(\omega+\omega') , \tag{3.26}$$

where

$$g_1(\omega)=\frac{\sinh 2r 32\Omega\kappa^2[(\gamma_b/2)^2+\Omega^2-\omega^2]I}{|\Lambda_1(\omega)|^2|\Lambda_3(\omega)|^2|\Lambda_4(\omega)|^2} , \tag{3.27}$$

$$g_2(\omega)=\sinh 2r\left[\frac{(16\Omega\kappa^2)^2I^2}{|\Lambda_1(\omega)|^4|\Lambda_3(\omega)|^2|\Lambda_4(\omega)|^2}-1\right] , \tag{3.28}$$

$$g_3(\omega)=\frac{16\kappa^2\gamma_b[(\gamma_b/2)^2+\Omega^2+\omega^2]I}{|\Lambda_1(\omega)|^2|\Lambda_3(\omega)|^2|\Lambda_4(\omega)|^2}+\cosh 2r\left[1+\frac{(16\Omega\kappa^2)^2I^2}{|\Lambda_1(\omega)|^4|\Lambda_3(\omega)|^2|\Lambda_4(\omega)|^2}\right] . \tag{3.29}$$

Optimizing Eq. (3.26) with respect to θ yields

$$\mathcal{V}^{\text{opt}}(\omega)=2I\{-[g_1^2(\omega)+g_2^2(\omega)]^{1/2}+g_3(\omega)\}\delta(\omega+\omega') , \tag{3.30}$$

where

$$\theta^{\text{opt}}(\omega)=\tan^{-1}\left[\frac{g_1(\omega)}{g_2(\omega)}\right] , \tag{3.31}$$

if $g_2(\omega)\neq 0$, or $\pi/2$ or $3\pi/2$ if $g_2(\omega)=0$.

The first, second, and fourth terms in Eq. (3.25) are the photon counting, mirror, and radiation pressure noise terms, respectively. Whereas the photon counting and radiation pressure noise terms are affected by the squeezing, the mirror noise is totally independent of the squeezing, which is in accord with the discussion in the preceding section on the physical origin of these terms. The third term in Eq. (3.25) is a correlation term which, unlike the other noise terms, can be either positive or negative. It corresponds to the S_{pq} correlation term appearing in Jaekel and Reynaud's paper [14]. The squeezed state with arbitrary squeezing phase [12] is a contractive state (as discussed by Yuen [7]) if this correlation term is negative.

From Eq. (3.25) it follows that amplitude squeezed light, and not phase squeezed, reduces the photon counting noise. This may seem counterintuitive in light of the preceding discussion, in which the photon counting noise was attributed to phase fluctuations of the light field inside the cavity. Figure 4 resolves this puzzle by showing

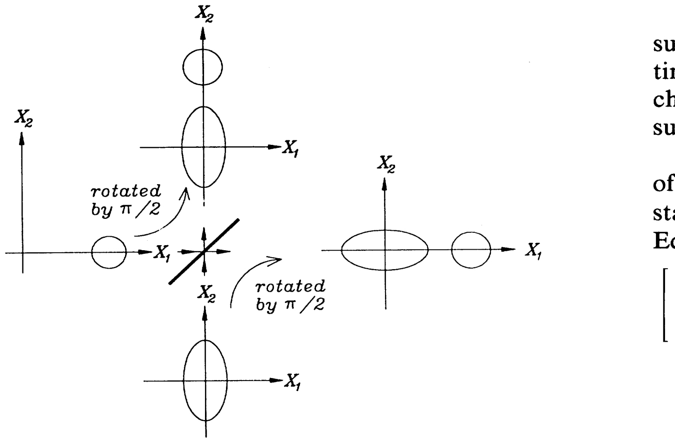

FIG. 4. Amplitude squeezed light on the outside looks like phase squeezed light inside the cavities.

why amplitude squeezed light entering the nonlaser input of the interferometer looks like phase squeezed light entering each cavity, relative to the phase of the coherent laser amplitude.

At this stage it is instructive to optimize h with respect to power keeping $\theta=0$ and to compare the results with those of Caves [11].

Writing the signal and variance in the form of Eqs. (2.52) and (2.53) for $\theta=0$, we get

$$f_s(\omega)=\frac{32\omega_g^2\omega_0 I}{\Lambda_1(\omega)\Lambda_3(\omega)\Lambda_4(\omega)} \tag{3.32}$$

and

$$f_v(\omega)=2I\left[e^{-2r}+\frac{16\kappa^2\gamma_b[(\gamma_b/2)^2+\Omega^2+\omega^2]I}{|\Lambda_1(\omega)|^2|\Lambda_3(\omega)|^2|\Lambda_4(\omega)|^2}+\frac{e^{2r}(16\Omega\kappa^2)^2I^2}{|\Lambda_1(\omega)|^4|\Lambda_3(\omega)|^2|\Lambda_4(\omega)|^2}\right], \tag{3.33}$$

from which it is clear that for $\theta=0$ there is no contribution from the correlation noise term. Substituting $f_s(\omega)$ and $f_v(\omega)$ back into Eq. (2.57) yields

$$h^2=f(\omega_g)[e^{-2r}/I+f_1(\omega_g)+f_2(\omega_g)e^{2r}I], \tag{3.34}$$

where $f(\omega)$, $f_1(\omega)$, and $f_2(\omega)$ are defined in Eqs. (2.72), (2.73), and (2.74). The minimum value of h^2 occurs for an optimum intensity

$$I_{\rm opt}=\frac{e^{-2r}}{[f_2(\omega_g)]^{1/2}} \tag{3.35}$$

and hence the optimum laser power is

$$P_{\rm opt}=2\hbar\omega_0 I_{\rm opt}=e^{-2r}P_0, \tag{3.36}$$

where P_0 is the optimum laser power for the system with no squeezing. Substituting $I_{\rm opt}$ back into Eq. (3.34) gives

$$h^2_{\rm min}=f(\omega_g)\{2[f_2(\omega_g)]^{1/2}+f_1(\omega_g)\}, \tag{3.37}$$

which is independent of the squeezing parameter r.

These results for $\theta=0$ agree qualitatively with the results of Caves [5]. Namely, the squeezing reduces the optimum laser power according to Eq. (3.36), but it does not change the detectability of h. Figure 5 displays these results using the same numerical data as for Fig. 3.

We now consider using squeezed light where the phase of the squeezing is given by $\theta_{\rm opt}$. The problem as it stands is analytically intractable, so the variance found in Eq. (3.30) must be simplified. Using the approximation

$$\left[\left[\frac{\gamma_b}{2}\right]^2+\Omega^2-\omega^2\right]^2-\omega^2\gamma_b^2 \approx \left[\left[\frac{\gamma_b}{2}\right]^2+\Omega^2-\omega^2\right]^2+\omega^2\gamma_b^2 \tag{3.38}$$

$$=|\Lambda_3(\omega)|^2|\Lambda_4(\omega)|^2, \tag{3.39}$$

which is valid in the high-frequency regime in which we are working, we get

$$[g_1^2(\omega)+g_2^2(\omega)]^{1/2}=|\sinh 2r|\left[1+\frac{(16\Omega\kappa^2)^2I^2}{|\Lambda_1(\omega)|^4|\Lambda_3(\omega)|^2|\Lambda_4(\omega)|^2}\right]. \tag{3.40}$$

Hence the variance can be written in the form of Eq. (2.53), where

$$f_v(\omega)=2I\left[e^{-2|r|}+\frac{16\kappa^2\gamma_b[(\gamma_b/2)^2+\Omega^2+\omega^2]I}{|\Lambda_1(\omega)|^2|\Lambda_3(\omega)|^2|\Lambda_4(\omega)|^2}+\frac{e^{-2|r|}(16\Omega\kappa^2)^2I^2}{|\Lambda_1(\omega)|^4|\Lambda_3(\omega)|^2|\Lambda_4(\omega)|^2}\right]. \tag{3.41}$$

So using Eq. (2.57) we get

$$h^2=f(\omega_g)[e^{-2|r|}/I+f_1(\omega_g)+f_2(\omega_g)e^{-2|r|}I], \tag{3.42}$$

where $f(\omega_g)$, $f_1(\omega_g)$, and $f_2(\omega_g)$ are defined in Eqs. (2.72), (2.73), and (2.74). We obtain a minimum in h^2 for an optimum intensity given by

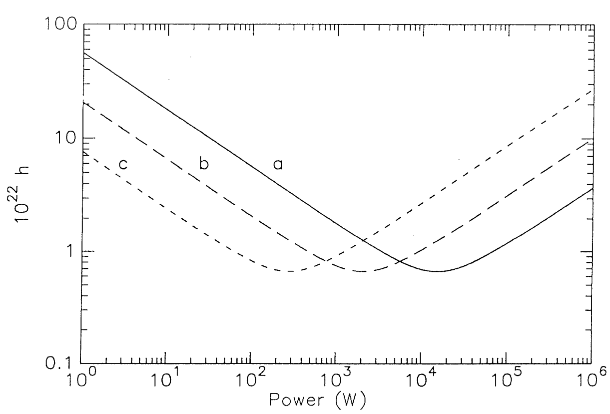

FIG. 5. The minimum possible gravitational wave amplitude h detectable as a function of power using $\theta=0$, for three different values of the squeezing parameter r: (curve a) $r=0$, (curve b) $r=1$, (curve c) $r=2$.

$$I_{\rm opt}=\frac{1}{[f_2(\omega_g)]^{1/2}} \quad (3.43)$$

$$\Longrightarrow P_{\rm opt}=2\hbar\omega_0 I_{\rm opt}=P_0 \ . \quad (3.44)$$

So the optimum laser power does not change with squeezing when $\theta=\theta_{\rm opt}$ is used. Inserting $I_{\rm opt}$ back into Eq. (3.42) gives

$$h^2_{\min}=f(\omega_g)\{2e^{-2|r|}[f_2(\omega_g)]^{1/2}+f_1(\omega_g)\} \quad (3.45)$$

$$\approx\frac{\hbar}{8M\omega_g^2L^2\tau\Omega}[2e^{-2|r|}\Omega+\gamma_b] \ , \quad (3.46)$$

where in the last line the approximation in Eq. (2.78) has been used.

Equation (3.42) gives us one way of viewing the correlation term. Its basic effect is to reduce the photon counting and radiation pressure noise terms by a factor of $e^{-2|r|}$, thus clearly beating the SQL. This viewpoint, which is valid for all laser powers, gives us insight into several things, as follows.

(i) The correlation term can never completely cancel out the effect of the light noise.

(ii) Since the light noise is effectively scaled by $e^{-2|r|}$, with increased squeezing it can be reduced to such a level that the mirror noise is dominant. So for highly squeezed states the interferometer is limited by the damping noise in the mirror. It is not possible for this particular experimental setup to get below the mirror noise.

(iii) The optimum power is independent of squeezing as the correlation term causes both the photon counting and radiation pressure noise terms to scale in exactly the same way.

(iv) The optimum phase at the optimum power is $\pi/2$. This corresponds to an error ellipse tilted at an angle of $\pi/4$ for the squeezed vacuum mode, c_2. This shows that because of the correlation term we desire an equal mix of the photon counting and radiation pressure noise terms in order to minimize h.

Figure 6 shows some of these points. It was obtained

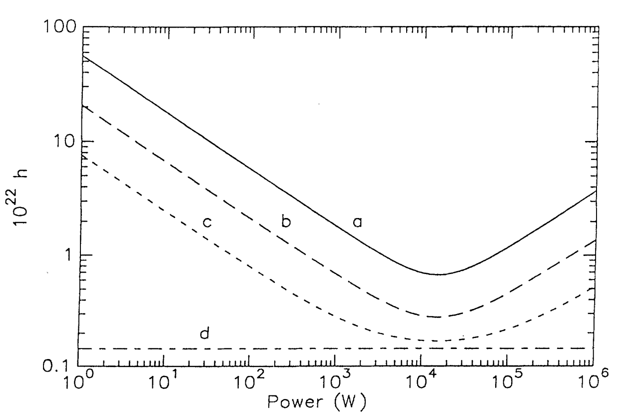

FIG. 6. The minimum possible value of h detectable as a function of power using $\theta^{\rm opt}$, for three different values of the squeezing parameter r: (curve a) $r=0$, (curve b) $r=1$, (curve c) $r=2$. The contribution of the mirror noise to h has also been drawn in (see curve d).

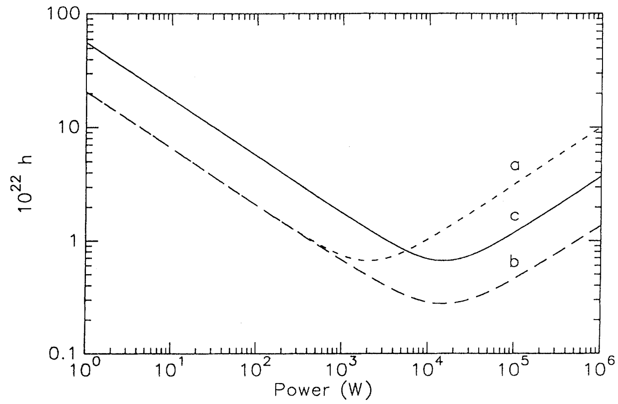

FIG. 7. A comparison between using (curve a) $\theta=0$ and (curve b) $\theta^{\rm opt}$, in the calculation for the minimum possible value of h detectable using $r=1$. The corresponding curve for no squeezing ($r=0$) is also shown (see curve c).

numerically from the exact expression for h^2 [i.e., not using the approximation in Eq. (2.78)].

Figure 7 compares our results using $\theta=0$ with those using $\theta=\theta^{\rm opt}$, for $r=1$. $\theta^{\rm opt}$ clearly beats the SQL while $\theta=0$ just reaches the SQL. The results using $\theta^{\rm opt}$ are always better than those for $\theta=0$, but for low powers there is practically no difference between the two because in that regime $\theta^{\rm opt}\approx 0$.

Our results agree with Unruh's work [12] which says that the light noise can be reduced by an arbitrary amount by using a squeezed state as input into the vacuum input port of the interferometer. Furthermore Unruh did not think that the damping fluctuations of the mirror were important except if the light was "strongly squeezed," which agrees qualitatively with our work. Jaekel and Reynaud [14] and Luis and Sanchez-Soto [15], while using different formalisms from Unruh, also obtained results which were significantly below the SQL and were limited by the mirror damping and not the light noise. These results also show that Yuen's work on contractive states [7] is applicable to gravitational wave interferometry and that these contractive states can be used to beat the SQL.

Extensions to include the use of squeezed light in the presence of phase modulation [23] and for nonideal interferometers [24] have been discussed.

IV. KERR MEDIUM

In this section we investigate the effect of placing a Kerr medium inside both cavities of the interferometer in the hope of beating the SQL. A Kerr medium has the property that it has an intensity-dependent refractive index. It has been noted by Loudon [6] that there is a similarity between a Kerr medium and radiation pressure in their effect on the cavity light field, namely, they both introduce a phase shift proportional to the intensity of the light. From this observation stemmed the idea [16] that if the sign and magnitude of the Kerr medium were carefully chosen, then it might completely cancel out the effect of the radiation pressure fluctuations, thus improving the sensitivity of the interferometer's measurement of h. The method is the same as before, so the notation introduced in Sec. II will remain unchanged.

A. The system and its solution

As in Sec. II, we are considering the external laser field detuned relative to the internal cavity resonance frequency and hence the internal cavity mode, a, will be treated in an interaction picture rotating at the laser frequency. The introduction of a Kerr medium into each cavity may be modeled by adding a term $\hbar\chi a^{\dagger 2}a^2$ to the Hamiltonian in Eq. (2.2). So $H_{\rm sys}$ becomes

$$H_{\rm sys}=\hbar\Delta a^\dagger a+\hbar\Omega b^\dagger b+\hbar\kappa a^\dagger a(b+b^\dagger)+\hbar k s(t)(b+b^\dagger)+\hbar\chi a^{\dagger 2}a^2 , \tag{4.1}$$

where χ is a constant proportional to $\chi^{(3)}$. The other terms and parameters are the same as before.

A quantum Langevin equation for each internal mode operator can now be written as

$$\dot a=-i[\Delta a+\kappa a(b+b^\dagger)+\chi 2a^\dagger a^2]-\frac{\gamma_a}{2}a+\gamma_a^{1/2}a^{\rm in} , \tag{4.2}$$

$$\dot b=-i[\Omega b+\kappa a^\dagger a+ks(t)]-\frac{\gamma_b}{2}b+\gamma_b^{1/2}b^{\rm in} , \tag{4.3}$$

where, as before, γ_a is the cavity field mode damping constant and γ_b is the mirror mode damping constant.

As in Sec. II, we can linearize Eqs. (4.2) and (4.3) about their semiclassical solutions. So setting all operators and parameters equal to their respective steady-state mean values we obtain

$$\alpha=\frac{\gamma_a^{1/2}\xi}{\gamma_a/2+i[\Delta+\kappa(\beta+\beta^*)+2\chi\alpha^*\alpha]} , \tag{4.4}$$

$$\beta=\frac{-i\kappa\alpha^*\alpha}{\gamma_b/2+i\Omega} , \tag{4.5}$$

where $\langle a\rangle=\alpha$, $\langle b\rangle=\beta$, $\langle b^{\rm in}\rangle=0$, and $\langle a^{\rm in}\rangle=\xi$, where ξ is the coherent driving field amplitude due to the laser.

In this problem we are free to choose the values of both Δ and χ. We shall always choose the detuning Δ so that

$$\Delta+\kappa(\beta+\beta^*)+2\chi\alpha^*\alpha=0 , \tag{4.6}$$

and then choose χ to give us the best sensitivity for our measurement of h. Physically this corresponds to choosing the detuning in such a way that the cavity is still on resonance.

Inserting Eq. (4.6) back into Eq. (4.4) gives

$$\alpha=\frac{2\xi}{\gamma_a^{1/2}} , \tag{4.7}$$

$$\beta=\frac{-4i\kappa|\xi|^2/\gamma_a}{\gamma_b/2+i\Omega} . \tag{4.8}$$

Now substituting the following back into Eqs. (4.2) and (4.3),

$$a=\alpha+\delta a , \quad b=\beta+\delta b , \quad a^{\rm in}=\xi+\delta a^{\rm in} , \quad b^{\rm in}=\delta b^{\rm in} , \tag{4.9}$$

and expanding to first order in the fluctuations [using Eq. (4.6)], we obtain the linearized equations of motion which in matrix form are

$$\frac{d}{dt}\begin{bmatrix}\delta a\\ \delta a^\dagger\\ \delta b\\ \delta b^\dagger\end{bmatrix}=-\begin{bmatrix}\frac{\gamma_a}{2}+2i\chi|\alpha|^2 & 2i\chi\alpha^2 & i\kappa\alpha & i\kappa\alpha\\ -2i\chi\alpha^{*2} & \frac{\gamma_a}{2}-2i\chi|\alpha|^2 & -i\kappa\alpha^* & -i\kappa\alpha^*\\ i\kappa\alpha^* & i\kappa\alpha & \frac{\gamma_b}{2}+i\Omega & 0\\ -i\kappa\alpha^* & -i\kappa\alpha & 0 & \frac{\gamma_b}{2}-i\Omega\end{bmatrix}\begin{bmatrix}\delta a\\ \delta a^\dagger\\ \delta b\\ \delta b^\dagger\end{bmatrix}+\begin{bmatrix}\sqrt{\gamma_a}\delta a^{\rm in}\\ \sqrt{\gamma_a}\delta a^{\rm in\dagger}\\ \sqrt{\gamma_b}\delta b^{\rm in}\\ \sqrt{\gamma_b}\delta b^{\rm in\dagger}\end{bmatrix}+\begin{bmatrix}0\\ 0\\ -iks(t)\\ +iks(t)\end{bmatrix} \tag{4.10}$$

$$\Longleftrightarrow\frac{d}{dt}\delta\mathbf{a}(t)=-\mathbf{A}\delta\mathbf{a}(t)+\mathbf{F}(t)+\mathbf{g}(t) . \tag{4.11}$$

Transforming Eq. (4.11) into the frequency domain using Eq. (2.13) yields

$$\delta\mathbf{a}(\omega)=(\mathbf{A}-i\omega\mathbf{I})^{-1}[\mathbf{F}(\omega)+g(\omega)] , \tag{4.12}$$

where

$$\mathbf{F}(\omega)=\begin{bmatrix}\gamma_a^{1/2}\delta a^{\text{in}}(\omega)\\ \gamma_a^{1/2}\delta a^{\text{in}\dagger}(\omega)\\ \gamma_b^{1/2}\delta b^{\text{in}}(\omega)\\ \gamma_b^{1/2}\delta b^{\text{in}\dagger}(\omega)\end{bmatrix},\quad \mathbf{g}(\omega)=iks(\omega)\begin{bmatrix}0\\0\\-1\\+1\end{bmatrix}, \tag{4.13}$$

and

$$(\mathbf{A}-i\omega\mathbf{I})^{-1}=(\mathbf{A}-i\omega\mathbf{I})_1^{-1} \tag{4.14}$$

$$=\begin{bmatrix}\frac{\Lambda_2\Lambda_3\Lambda_4+2i\Omega\kappa^2|\alpha|^2}{\Lambda_1^2\Lambda_3\Lambda_4} & \frac{-2i\alpha^2(\chi\Lambda_3\Lambda_4-\Omega\kappa^2)}{\Lambda_1^2\Lambda_3\Lambda_4} & \frac{-i\kappa\alpha}{\Lambda_1\Lambda_3} & \frac{-i\kappa\alpha}{\Lambda_1\Lambda_4}\\ \frac{2i\alpha^{*2}(\chi\Lambda_3\Lambda_4-\Omega\kappa^2)}{\Lambda_1^2\Lambda_3\Lambda_4} & \frac{\Lambda_0\Lambda_3\Lambda_4-2i\Omega\kappa^2|\alpha|^2}{\Lambda_1^2\Lambda_3\Lambda_4} & \frac{i\kappa\alpha^*}{\Lambda_1\Lambda_3} & \frac{i\kappa\alpha^*}{\Lambda_1\Lambda_4}\\ \frac{-i\kappa\alpha^*}{\Lambda_1\Lambda_3} & \frac{-i\kappa\alpha}{\Lambda_1\Lambda_3} & \frac{1}{\Lambda_3} & 0\\ \frac{i\kappa\alpha^*}{\Lambda_1\Lambda_4} & \frac{i\kappa\alpha}{\Lambda_1\Lambda_4} & 0 & \frac{1}{\Lambda_4}\end{bmatrix}, \tag{4.15}$$

where

$$\Lambda_0\equiv\Lambda_0(\omega)=\frac{\gamma_a}{2}+i(2\chi|\alpha|^2-\omega), \tag{4.16}$$

$$\Lambda_1\equiv\Lambda_1(\omega)=\frac{\gamma_a}{2}-i\omega, \tag{4.17}$$

$$\Lambda_2\equiv\Lambda_2(\omega)=\frac{\gamma_a}{2}-i(2\chi|\alpha|^2+\omega), \tag{4.18}$$

$$\Lambda_3\equiv\Lambda_3(\omega)=\frac{\gamma_b}{2}+i(\Omega-\omega), \tag{4.19}$$

$$\Lambda_4\equiv\Lambda_4(\omega)=\frac{\gamma_b}{2}-i(\Omega+\omega). \tag{4.20}$$

The $b_{ij}(\omega)$ remain defined by Eq. (2.21), where $(\mathbf{A}-i\omega\mathbf{I})_1^{-1}$ is now given by Eq. (4.15).

Comparing Eqs. (2.17)–(2.20) with Eqs. (4.15)–(4.20), we see that the two matrices are exactly equal apart from the 2×2 submatrix in the upper left-hand corner, that is, apart from the terms b_{11}, b_{12}, b_{21}, and b_{22}.

B. Calculating the signal and variance

Now the next step is to combine the contributions from both cavities. Equations (2.22)–(2.32) and the accompanying comments, hold equally true here for the Kerr medium case. Our input light fields, c_1 and c_2 (see Fig. 1), are a coherent state (laser input) and an unsqueezed vacuum, respectively. The mirror inputs, δb_1^{in} and δb_2^{in}, will also be assumed to be unsqueezed vacuum states. The input light fields are independent of the mirror inputs. As before, the thermal fluctuations in all the input field correlations will be neglected. With these assumptions, $\delta\mathbf{a}_1^{\text{in}}$ and $\delta\mathbf{a}_2^{\text{in}}$ are independent of each other:

$$\langle\delta\mathbf{a}_1^{\text{in}}(\omega)\delta\mathbf{a}_2^{\text{in}T}(\omega')\rangle=\langle\delta\mathbf{a}_2^{\text{in}}(\omega)\delta\mathbf{a}_1^{\text{in}T}(\omega')\rangle=\mathbf{0}, \tag{4.21}$$

and the other correlations are

$$\langle\delta\mathbf{a}_1^{\text{in}}(\omega)\delta\mathbf{a}_1^{\text{in}T}(\omega')\rangle=\langle\delta\mathbf{a}_2^{\text{in}}(\omega)\delta\mathbf{a}_2^{\text{in}T}(\omega')\rangle=\begin{bmatrix}0&1&0&0\\0&0&0&0\\0&0&0&1\\0&0&0&0\end{bmatrix}\delta(\omega+\omega'). \tag{4.22}$$

The following results are obtained for the components of $\mathbf{C}(\omega)$:

$$c_{11}=-c_{33}=\{[\gamma_a b_{11}(\omega)-1]\gamma_a b_{12}(\omega')+\gamma_a\gamma_b b_{13}(\omega)b_{14}(\omega')\}\delta(\omega+\omega'), \tag{4.23}$$

$$c_{12}=c_{34}=\{[\gamma_a b_{11}(\omega)-1][\gamma_a b_{22}(\omega')-1]+\gamma_a\gamma_b b_{13}(\omega)b_{24}(\omega')\}\delta(\omega+\omega'), \tag{4.24}$$

$$c_{21}=c_{43}=[\gamma_a^2 b_{21}(\omega)b_{12}(\omega')+\gamma_a\gamma_b b_{23}(\omega)b_{14}(\omega')]\delta(\omega+\omega'), \tag{4.25}$$

$$c_{22}=-c_{44}=\{\gamma_a b_{21}(\omega)[\gamma_a b_{22}(\omega')-1]+\gamma_a\gamma_b b_{23}(\omega)b_{24}(\omega')\}\delta(\omega+\omega'), \tag{4.26}$$

$$c_{13}=c_{14}=c_{23}=c_{24}=c_{31}=c_{32}=c_{41}=c_{42}=0. \tag{4.27}$$

Using the large intensity approximation Eq. (2.44) our signal is

$$\mathcal{S}(\omega)=\langle I_1(\omega)-I_2(\omega)\rangle \tag{4.28}$$

$$=2(I\gamma_a)^{1/2}ks(\omega)[b_{14}(\omega)-b_{13}(\omega)+b_{23}(\omega)-b_{24}(\omega)] \tag{4.29}$$

$$=\frac{32\hbar\omega_g^2\omega_0 s(\omega)I}{\Lambda_1(\omega)\Lambda_3(\omega)\Lambda_4(\omega)}, \quad (4.30)$$

where the $\Lambda_i(\omega)$ are defined in Eqs. (4.16)–(4.20). The signal is independent of χ and is identical to the signal found in Sec. II [see Eq. (2.47)]. We do indeed expect the gravity wave interaction to be independent of both the squeezing and Kerr medium.

Using Eq. (2.44) together with Eqs. (4.23)–(4.27) and (4.15), we get the following result for the variance:

$$\mathcal{V}=\langle I_1(\omega)-I_2(\omega), I_1(\omega')-I_2(\omega')\rangle \quad (4.31)$$

$$=2I[c_{12}+c_{21}-(c_{11}+c_{22})] \quad (4.32)$$

$$=2I\left[1+\frac{16\kappa^2\gamma_b[(\gamma_b/2)^2+\Omega^2+\omega^2]I}{|\Lambda_1(\omega)|^2|\Lambda_3(\omega)|^2|\Lambda_4(\omega)|^2}+\frac{f(\chi)}{|\Lambda_1(\omega)|^4|\Lambda_3(\omega)|^2|\Lambda_4(\omega)|^2}\right]\delta(\omega+\omega'), \quad (4.33)$$

where

$$f(\chi)=16^2I^2\{\chi^2|\Lambda_3(\omega)|^2|\Lambda_4(\omega)|^2-2\chi\Omega\kappa^2[(\gamma_b/2)^2+\Omega^2-\omega^2]+(\Omega\kappa^2)^2\} \quad (4.34)$$

$$=16^2I^2|\chi\Lambda_3(\omega)\Lambda_4(\omega)-\Omega\kappa^2|^2. \quad (4.35)$$

As the signal is independent of χ, in order to optimize the system with respect to the free parameter χ we need to minimize the variance. Fortunately the expression for the variance in Eq. (4.33) has only one term which depends on χ. We find for the minimum variance

$$\mathcal{V}^{\min}(\omega)=2I\left[1+\frac{16\kappa^2\gamma_b[(\gamma_b/2)^2+\Omega^2+\omega^2]I}{|\Lambda_1(\omega)|^2|\Lambda_3(\omega)|^2|\Lambda_4(\omega)|^2}+\frac{(16\gamma_b\kappa^2\Omega\omega)^2I^2}{|\Lambda_1(\omega)|^4|\Lambda_3(\omega)|^4|\Lambda_4(\omega)|^4}\right]\delta(\omega+\omega'), \quad (4.36)$$

which occurs for

$$\chi=\chi_{\rm opt}(\omega)=\frac{\Omega\kappa^2[(\gamma_b/2)^2+\Omega^2-\omega^2]}{|\Lambda_3(\omega)|^2|\Lambda_4(\omega)|^2}. \quad (4.37)$$

It is interesting to note that $\chi_{\rm opt}$ is independent of power. This is to be expected physically since the whole point of using a Kerr medium was to cancel out the effects of power fluctuations, independent of the size of these fluctuations. It can also be seen that the sign of $\chi_{\rm opt}$ depends on the frequency. For high frequencies $\chi_{\rm opt}$ is negative, corresponding to a "normal" Kerr medium (see Appendix D). In Bondurant's analysis [16] the Kerr medium required did not change sign and was always equivalent to χ being positive, that is, an anomalous Kerr medium. This discrepancy can be traced back to the fact that although Bondurant treated the mirror quantum mechanically, he did not specifically treat it as a damped harmonic oscillator. As the mirror acts like a damped, forced harmonic oscillator, at high frequencies the mirror displacement and radiation pressure fluctuations are almost *out of phase*, hence $\chi_{\rm opt}$ is negative.

Comparing our expression for the optimum variance for the Kerr medium (4.36) with the variance without the Kerr medium [i.e., set $\chi=0$ in Eq. (4.33)], we see that the Kerr medium reduces the radiation pressure noise while leaving the mirror noise and photon counting noise unchanged. There is complete cancellation of the radiation pressure noise only when the mirror displacement and the radiation pressure fluctuations are either exactly in phase or exactly out of phase. Although this condition is never exactly met at finite, nonzero frequencies, the radiation pressure noise can be very much reduced.

C. Evaluating the performance

The next step is to optimize the power. The signal and variance can be written in the form of Eqs. (2.52) and (2.53), where

$$f_s(\omega)=\frac{32\omega_g^2\omega_0 I}{\Lambda_1(\omega)\Lambda_3(\omega)\Lambda_4(\omega)} \quad (4.38)$$

and

$$f_v(\omega)=2I\left[1+\frac{16\kappa^2\gamma_b[(\gamma_b/2)^2+\Omega^2+\omega^2]I}{|\Lambda_1(\omega)|^2|\Lambda_3(\omega)|^2|\Lambda_4(\omega)|^2}+\frac{(16\gamma_b\kappa^2\Omega\omega)^2I^2}{|\Lambda_1(\omega)|^4|\Lambda_3(\omega)|^4|\Lambda_4(\omega)|^4}\right]. \quad (4.39)$$

So using Eq. (2.57) we get

$$h^2=f(\omega_g)[1/I+f_1(\omega_g)+f_2(\omega_g)I], \quad (4.40)$$

where

$$f(\omega)=\frac{|\Lambda_1(\omega)|^2|\Lambda_3(\omega)|^2|\Lambda_4(\omega)|^2}{\tau[16\omega_g^2\omega_0]^2}, \quad (4.41)$$

$$f_1(\omega)=\frac{16\kappa^2\gamma_b[(\gamma_b/2)^2+\Omega^2+\omega^2]}{|\Lambda_1(\omega)|^2|\Lambda_3(\omega)|^2|\Lambda_4(\omega)|^2}, \quad (4.42)$$

$$f_2(\omega)=\frac{(16\gamma_b\kappa^2\Omega\omega)^2}{|\Lambda_1(\omega)|^4|\Lambda_3(\omega)|^4|\Lambda_4(\omega)|^4}. \quad (4.43)$$

By differentiation we find a minimum in h^2 at

$$I_{\rm opt}=\frac{1}{[f_2(\omega_g)]^{1/2}} \quad (4.44)$$

$$=\frac{|\Lambda_1(\omega_g)|^2|\Lambda_3(\omega_g)|^2|\Lambda_4(\omega_g)|^2}{16\gamma_b\kappa^2\Omega\omega_g}, \quad (4.45)$$

corresponding to an optimum laser power of

$$P_1=2\hbar\omega_0 I_{\rm opt}. \quad (4.46)$$

Comparing this with the optimum power obtained in Eq. (2.76), P_0, and realizing that we are in the frequency regime in which $\omega_g^2 \gg (\gamma_b/2)^2+\Omega^2$, we get

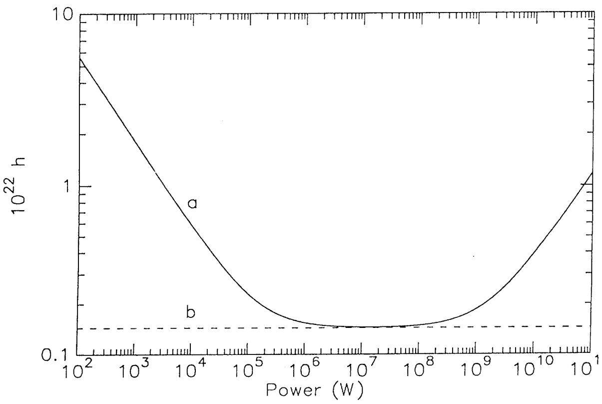

FIG. 8. (Curve *a*) The minimum possible gravitational wave amplitude *h* detectable as a function of power using a Kerr medium. (Curve *b*) The contribution of the mirror noise to *h*.

$$\frac{P_1}{P_0} \approx \frac{\omega_g}{\gamma_b} \gg 1 \ . \tag{4.47}$$

Inserting I_{opt} back into the expression for h^2 (4.40) gives

$$h_{\min}^2 = f(\omega_g)\{2[f_2(\omega_g)]^{1/2} + f_1(\omega_g)\} \tag{4.48}$$

$$= \frac{\hbar\gamma_b}{8M\omega_g^4 L^2 \tau\Omega}\left[2\Omega\omega_g + \left[\frac{\gamma_b}{2}\right]^2 + \Omega^2 + \omega_g^2\right] \tag{4.49}$$

$$\approx \frac{\hbar\gamma_b}{8M\omega_g^2 L^2\tau\Omega} \ , \tag{4.50}$$

where in the last line we have noted that in the high-frequency regime in which we are interested we have

$$\omega_g^2 \gg \left[\frac{\gamma_b}{2}\right]^2 + \Omega^2 + 2\Omega\omega_g \ . \tag{4.51}$$

The first term in the square brackets in Eq. (4.49) can be traced back to the quantum-mechanical uncertainties in the light. This term is now insignificant compared to the mirror noise, which is unchanged from Eq. (3.37) and which consists of the remaining terms in Eq. (4.49). Thus the inclusion of the Kerr medium into each cavity significantly reduces $h_{\min}^2$ and hence beats the SQL. This minimum in h occurs at a much higher laser power than before [see Eq. (4.47)], simply because the effect of the Kerr medium is to reduce the radiation pressure noise, which means that the photon counting noise and radiation pressure noise are equal (and hence minimum) at a much higher laser power. Figure 8 highlights the point that h is limited by the mirror noise, as opposed to the light noise, and that this minimum in h occurs at a very large laser power. Bondurant in his analysis did not treat the mirror as a damped harmonic oscillator, hence he was able to nullify the radiation pressure noise at a particular frequency (though not over a finite bandwidth) and he did not get a mirror noise term.

V. CONCLUSIONS

The physical origin of the interferometer noise sources was explained from the perspective that an interferometer simply detects phase fluctuations of the light inside the cavity. In particular, the photon counting noise is due to phase fluctuations in the light entering the cavity, and the radiation pressure noise is due to intensity fluctuations in the light entering the cavity—these produce fluctuations in the mirror displacement, which in turn produce phase changes in the cavity light field.

Either the photon counting or the radiation pressure fluctuations may be reduced by injecting phase or amplitude squeezed light into the empty port of the interferometer, as shown by Caves. However, a reduction of both noise sources can be achieved by using a squeezed state with negative correlations between the quadratures. By choosing the optimum phase of the squeezing, reductions below the SQL for h can be obtained. The light noise, with sufficient squeezing, can be reduced to an insignificant level compared to the mirror noise (which is independent of the squeezing). The laser power required to get the best sensitivity in the measurement of h does not change with squeezing.

The effect of including the Kerr medium is to reduce the radiation pressure fluctuations, but there is not complete cancellation due to a phase lag in the response of the mirror to the light field driving it. Reductions below the SQL for h can be obtained but a higher laser power, relative to the squeezing case, is required in order to get the best sensitivity in the measurement of h. The sign of the Kerr medium required is negative, corresponding to a normal Kerr medium, not an anomalous one. The system is limited ultimately not by fluctuations in the light but by the damping noise in the mirrors.

ACKNOWLEDGMENTS

This research has been supported by the University of Auckland Research Committee, the New Zealand Vice Chancellor Committee, the New Zealand Lottery Grants Board, IBM New Zealand, and the U.S. Office of Naval Research.

APPENDIX A: DERIVATION OF κ

In this appendix we show just one of a variety of possible ways of deriving the radiation pressure coupling constant κ in terms of the parameters of the system.

Consider a cavity of length L with a cavity resonance frequency of ω_0. Then the Hamiltonian for the light resonant inside the cavity is

$$H = \hbar\omega_0 a^\dagger a \ . \tag{A1}$$

Now we have

$$\omega_0 = (n + \tfrac{1}{2})\omega_f \ , \tag{A2}$$

where n is integral or half-integral and ω_f is the fundamental cavity frequency:

$$\omega_f = \frac{2\pi c}{L} \ . \tag{A3}$$

Therefore Eq. (A1) can be written as

$$H=\hbar(n+\tfrac{1}{2})\frac{2\pi c}{L}a^{\dagger}a \; . \tag{A4}$$

Now if the mirror moves so that the length of the cavity is increased from L to $L+x$, this decreases the fundamental cavity frequency to ω'_f. So Eq. (A4) becomes

$$H=\hbar(n+\tfrac{1}{2})\frac{2\pi c}{L+x}a^{\dagger}a \; . \tag{A5}$$

But from Eq. (A3) we have

$$2\pi c=\omega_f L \; , \tag{A6}$$

where ω_f is the original fundamental cavity frequency. So

$$H=\hbar(n+\tfrac{1}{2})\omega_f\frac{L}{L+x}a^{\dagger}a \; , \tag{A7}$$

$$H\approx\hbar\omega_0\left[1-\frac{x}{L}\right]a^{\dagger}a \tag{A8}$$

$$\approx\hbar\omega_0 a^{\dagger}a-\hbar\frac{\omega_0}{L}a^{\dagger}ax \; , \tag{A9}$$

where in Eq. (A8) we have assumed x small. The last term in Eq. (A9) shows how the intracavity energy changes as the mirror moves, which is the radiation pressure energy term.

This derivation assumes that x does not move a significant fraction of a wavelength in one cavity round-trip time; if it did there would be Doppler-induced scattering into other cavity modes. We are certainly justified in ignoring this for the parameters given in Table I.

Now quantizing the mirror position x we get

$$x=\left[\frac{2\hbar}{M\Omega}\right]^{1/2}(b+b^{\dagger}) \; , \tag{A10}$$

where M is the mass of the mirror and Ω is its characteristic frequency. Substituting Eq. (A10) back into the radiation pressure energy term in Eq. (A9) gives

$$H_{\rm rp}=-\hbar\frac{\omega_0}{L}a^{\dagger}a\left[\frac{2\hbar}{M\Omega}\right]^{1/2}(b+b^{\dagger}) \; . \tag{A11}$$

Comparing this with the radiation pressure energy term used in this paper,

$$H_{\rm rp}=\hbar\kappa a^{\dagger}a(b+b^{\dagger}) \; , \tag{A12}$$

we see that

$$\kappa=-\frac{\omega_0}{L}\left[\frac{2\hbar}{M\Omega}\right]^{1/2} \; . \tag{A13}$$

APPENDIX B: DERIVATION OF k

In this appendix we derive an expression for k in terms of the experimental parameters of the system and the gravity wave amplitude h.

The force on the mirror due to the gravity wave is

$$F_{\rm gravity}(t)=Mg(t) \; , \tag{B1}$$

where M is the mass of the mirror and $g(t)$ is the acceleration of the mirror due to the gravity wave. In this paper it is assumed that the gravity wave, in the absence of all other forces, displaces the mirror sinusoidally in time. Therefore the acceleration is

$$g(t)=gs(t) \; , \tag{B2}$$

where g is a constant to be determined and

$$s(t)=\cos(\omega_g t) \; , \tag{B3}$$

where ω_g is the gravity wave angular frequency.

Integrating $s(t)$ twice, we get for the displacement of the mirror, $x(t)$:

$$x(t)=-\frac{gs(t)}{\omega_g^2} \; . \tag{B4}$$

Now the gravitational wave amplitude h is defined to be the maximum fractional change in the cavity length L produced by the gravity wave in the absence of all other forces acting. So

$$h=\frac{\max(x(t))}{L}=\frac{-g}{L\omega_g^2} \; . \tag{B5}$$

Therefore using Eqs. (B1) and (B5) the gravity wave energy term can be written as

$$H_{\rm gravity}(t)=F_{\rm gravity}(t)x(t) \tag{B6}$$

$$=-MhL\omega_g^2 s(t)x(t) \tag{B7}$$

$$=-MhL\omega_g^2 s(t)\left[\frac{2\hbar}{M\Omega}\right]^{1/2}(b+b^{\dagger}) \; , \tag{B8}$$

where in the last line the mirror position, $x(t)$, has been quantized using Eq. (A10). Comparing this with the gravity wave energy term used in this paper,

$$H_{\rm gravity}(t)=\hbar ks(t)(b+b^{\dagger}) \; , \tag{B9}$$

we see that

$$k=-\left[\frac{2M}{\hbar\Omega}\right]^{1/2}hL\omega_g^2 \; . \tag{B10}$$

APPENDIX C: EXPRESSION FOR γ_a

We wish to express γ_a in terms of the cavity parameters. We have a cavity of length L enclosed by two mirrors M_1 and M_2. M_1 has a reflectivity R and a cavity damping constant γ_a, while M_2 is assumed to be perfectly reflecting.

The cavity damping constant γ_a is simply the reciprocal of t_c, the mean cavity lifetime of a photon. A photon has a round-trip time inside the cavity of $2L/c$ and each time it hits the mirror M_1 it has a probability of $T=1-R$ of being transmitted and exiting the cavity. Therefore a photon has a probability of $(1-R)R^{i-1}$ of having a cavity lifetime of i times the round-trip time. So

$$t_c=\sum_{i=1}^{\infty} i \left[\frac{2L}{c} \right] (1-R)R^{i-1} \tag{C1}$$

$$=\frac{2L}{c}\frac{1}{1-R} \tag{C2}$$

and hence

$$\gamma_a=\frac{1}{t_c}=\frac{c(1-R)}{2L} \ . \tag{C3}$$

APPENDIX D: COMMENTS ABOUT THE SIGN OF χ

The Hamiltonian for a medium with a $\chi^{(3)}$ nonlinearity is usually expressed in the form

$$H=\frac{1}{2}\int \left[\epsilon \mathbf{E}^2+\frac{\mathbf{B}^2}{\mu_0} \right] d\mathbf{r} \ , \tag{D1}$$

where the dielectric constant ϵ is

$$\epsilon=\epsilon_0(1+\chi^{(3)}\mathbf{E}^2) \ . \tag{D2}$$

Strictly speaking [25], the Hamiltonian should be written in terms of the electric displacement vector $\mathbf{D}$ (the conjugate momentum of $\mathbf{A}$) and not the electric field vector $\mathbf{E}$ (the conjugate velocity of $\mathbf{A}$), where $\mathbf{D}=\epsilon\mathbf{E}$,

$$H=\tfrac{1}{2}\int \left[\frac{\mathbf{D}^2}{\epsilon}+\frac{\mathbf{B}^2}{\mu_0} \right] d\mathbf{r} \ . \tag{D3}$$

For $\chi^{(3)}\mathbf{E}^2$ small compared with 1 we have

$$\frac{1}{\epsilon}\approx\frac{1}{\epsilon_0}(1-\chi^{(3)}\mathbf{E}^2)\approx\frac{1}{\epsilon_0}(1-\chi^{(3)}\epsilon_0^{-2}\mathbf{D}^2) \ , \tag{D4}$$

and hence, for a single mode analysis,

$$H=\tfrac{1}{2}\int \left[\frac{\mathbf{D}^2}{\epsilon_0}(1-\chi^{(3)}\epsilon_0^{-2}\mathbf{D}^2)+\frac{\mathbf{B}^2}{\mu_0} \right] d\mathbf{r} \tag{D5}$$

$$\equiv\hbar\omega_0(a^\dagger a+\tfrac{1}{2})+\hbar\chi a^{\dagger 2}a^2 \ . \tag{D6}$$

Comparing Eq. (D5) with Eq. (D6) we see that χ negative corresponds to $\chi^{(3)}$ positive, which is a *normal* Kerr medium; conversely, χ positive corresponds to an anomalous Kerr medium.

---

*Permanent address: Department of Physics, University of Auckland, Private Bag 92019, New Zealand.

[1] C. M. Caves, Phys. Rev. Lett. **54**, 2465 (1985).
[2] V. B. Brainsky and Yu. I. Vorontsov, Usp. Fiz. Nauk **114**, 41 (1974) [Sov. Phys. Usp. **17**, 644 (1975)].
[3] C. M. Caves, K. S. Thorne, R. W. P. Drever, V. D. Sandberg, and M. Zimmermann, Rev. Mod. Phys. **52**, 341 (1980).
[4] W. A. Edelstein, J. Hough, J. R. Pugh, and W. Martin, J. Phys. E **11**, 710 (1978).
[5] C. M. Caves, Phys. Rev. Lett. **45**, 75 (1980).
[6] R. Loudon, Phys. Rev. Lett. **47**, 815 (1981).
[7] H. P. Yuen, Phys. Rev. Lett. **51**, 719 (1983).
[8] W.-T. Ni, Phys. Rev. A **33**, 2225 (1986).
[9] M. Ozawa, Phys. Rev. A **41**, 1735 (1990).
[10] M. Ozawa, Phys. Rev. Lett. **60**, 385 (1988).
[11] C. M. Caves, Phys. Rev. D **23**, 1693 (1981).
[12] W. G. Unruh, in *Quantum Optics, Experimental Gravitation and Measurement Theory,* edited by P. Meystre and M. O. Scully (Plenum, New York, 1983), p. 647.
[13] R. S. Bondurant and J. H. Shapiro, Phys. Rev. D **30**, 2548 (1984).
[14] M. T. Jaekel and S. Reynaud, Europhys. Lett. **13**, 301 (1990).
[15] A. Luis and L. L. Sánchez-Soto, Phys. Rev. A **45**, 8228 (1992).
[16] R. S. Bondurant, Phys. Rev. A **34**, 3927 (1986).
[17] M. J. Collett and C. W. Gardiner, Phys. Rev. A **30**, 1386 (1984).
[18] C. W. Gardiner and M. J. Collett, Phys. Rev. A **31**, 3761 (1985).
[19] C. W. Helstrom, *Statistical Theory of Signal Detection* (Pergamon, Oxford, 1960).
[20] R. J. Glauber, Phys. Rev. **131**, 2766 (1963).
[21] D. Stoler, Phys. Rev. D **1**, 3217 (1970).
[22] J. N. Hollenhorst, Phys. Rev. D **19**, 1669 (1979).
[23] J. Gea-Banacloche and G. Leuchs, J. Mod. Opt. **34**, 793 (1987).
[24] J. Gea-Banacloche and G. Leuchs, J. Opt. Soc. Am. B **4**, 1667 (1987).
[25] R. J. Glauber and M. Lewenstein, Phys. Rev. A **43**, 467 (1991).